Detector response in the buildup region of small MV fields

Sonja Wegener[a)]
Department of Radiation Oncology, University of Wuerzburg, Josef-Schneider-Str. 11, 97080, Wuerzburg, Germany

Barbara Herzog
Department of Radiation Oncology, University of Wuerzburg, Josef-Schneider-Str. 11, 97080, Wuerzburg, Germany
Institute of Physics, Martin-Luther-Universität Halle-Wittenberg, Von-Danckelmann-Platz 3, 06120, Halle (Saale), Germany

Otto A. Sauer
Department of Radiation Oncology, University of Wuerzburg, Josef-Schneider-Str. 11, 97080, Wuerzburg, Germany

(Received 17 October 2018; revised 11 December 2019; accepted for publication 11 December 2019; published 20 January 2020)

Purpose: The model used to calculate dose distributions in a radiotherapy treatment plan relies on the data entered during beam commissioning. The quality of these data heavily depends on the detector choice made, especially in small fields and in the buildup region. Therefore, it is necessary to identify suitable detectors for measurements in the buildup region of small fields. To aid the understanding of a detector's limitations, several factors that influence the detector signal are to be analyzed, for example, the volume effect due to the detector size, the response to electron contamination, the signal dependence on the polarity used, and the effective point of measurement chosen.
Methods: We tested the suitability of different small field detectors for measurements of depth dose curves with a special focus on the surface-near area of dose buildup for fields sized between 10 × 10 and 0.6 × 0.6 cm^2. Depth dose curves were measured with 14 different detectors including plane-parallel chambers, thimble chambers of different types and sizes, shielded and unshielded diodes as well as a diamond detector. Those curves were compared with depth dose curves acquired on Gafchromic film. Additionally, the magnitude of geometric volume corrections was estimated from film profiles in different depths. Furthermore, a lead foil was inserted into the beam to reduce contaminating electrons and to study the resulting changes of the detector response. The role of the effective point of measurement was investigated by quantifying the changes occurring when shifting depth dose curves. Last, measurements for the small ionization chambers taken at opposing biasing voltages were compared to study polarity effects.
Results: Depth-dependent correction factors for relative depth dose curves with different detectors were derived. Film, the Farmer chamber FC23, a 0.13 cm^3 scanning chamber CC13 and a plane-parallel chamber PPC05 agree very well in fields sized 4 × 4 and 10 × 10 cm^2. For most detectors and in smaller fields, depth dose curves differ from the film. In general, shielded diodes require larger corrections than unshielded diodes. Neither the geometric volume effect nor the electron contamination can account for the detector differences. The biggest uncertainty arises from the positioning of a detector with respect to the water surface and from the choice of the detector's effective point of measurement. Depth dose curves acquired with small ionization chambers differ by over 15% in the buildup region depending on sign of the biasing voltage used.
Conclusions: A scanning chamber or a PPC40 chamber is suitable for fields larger than 4 × 4 cm^2. Below that field size, the microDiamond or small ionization chambers perform best requiring the smallest corrections at depth as well as in the buildup region. Diode response changes considerably between the different types of detectors. The position of the effective point of measurement has a huge effect on the resulting curves, therefore detector specific rather than general shifts of half the inner radius of cylindrical ionization chambers for the effective point of measurement should be used. For small ionization chambers, averaging between both polarities is necessary for data obtained near the surface. © *2019 The Authors. Medical Physics published by Wiley Periodicals, Inc. on behalf of American Association of Physicists in Medicine.* [https://doi.org/10.1002/mp.13973]

Key words: buildup region, diode, dosimetry, microionization chambers, percent depth dose curves

1. INTRODUCTION

Dose distributions for radiotherapy treatment plans need to be calculated with reasonable accuracy. In the buildup region or at the surface, dose measurement and calculations can deviate by over 10%.[1,2] Possible reasons are limitations of the calculation algorithms used and the challenges of beam modeling in the buildup region.[3,4] Any modeling depends on the quality of the measured data entered in the first place.

Dosimetry is especially challenging whenever a detector is placed in a region that does not provide charged particle equilibrium. The best known example for such a situation is the

measurement in small fields, where detector characteristics heavily influence their response.[5] Similarly, a photon beam incident on a water surface will create a gradient region, in which both the abundance and the energy spectrum of charged particles change rapidly, that is the buildup region of the depth dose curve.

Measurements at the surface and in the buildup region are not straightforward.[4,6,7] Ideally, one would like to measure with an infinitely thin detector preventing averaging over the detector's active volume. Any energy-dependent response is a concern in the buildup region, where low-energy photons are more abundant than at depth and where additional electron contamination generated in accelerator parts[8] or in air[9] is present.

An extrapolation chamber is a good choice of a detector at the surface.[10] However, those detectors' electrode spacing needs to be varied during the measurements, so they are more cumbersome to use than other detectors typically used for scanning, and not readily available. Measurements near the surface and in the buildup region are typically performed using plane-parallel chambers,[10] Their lateral dimensions can make those typically larger detectors unsuitable for measurements in small fields or in high gradient regions, where volume averaging becomes a concern. In that case, it seems logical to substitute plane-parallel with small field detectors. For profile and output factor measurements and especially for small field applications, a lot of different detector types are available.[5] Small field recommendations, such as TRS 483, state only general detector characteristics for relative dosimetry and some rough general guidelines.[5] However, the code of practice does not provide data on appropriate detector choices for depth dose curves and in the buildup region.

There have been several studies comparing different detector types for measurements including the buildup region.[11–15] The scintillator Exradin W1 was shown to produce depth dose curves in water in close agreement to Monte Carlo calculated curves.[11] This detector requires very careful measurements and does not easily allow scanning. Francescon et al.[11] stated a stereotactic diode as one of the reasonable choices for practical applications. They found systematic errors of percent depth dose curves (PDD) measured with that diode of <2% compared to the simulated depth dose curve in water in the absence of the detector. In a more recent work,[16] the same author recommended the microDiamond for requiring depth dose corrections $k_\Omega(0, z, PDD) < 1\%$ at all depths in all studied rectangular fields from 7.6×7.7 to 115×100.1 mm^2 with a CyberKnife 6 MV system. Scherf et al.[12] recommended the natural Diamond detector PTW 60003 for measurements both in the buildup region and the fall-off region of small photon beams. The studied shielded and unshielded diode and a PTW 233642 thimble chamber (0.125 cm^3 volume) showed restrictions in at least one of the regions.

Still, further investigations are necessary to understand the behavior of different detectors in the buildup region, especially in the surface-near region of small photon beams. This should help to choose appropriate detectors for measurements in small fields near the surface. We compared depth dose curves of different detectors with a focus on the buildup region to curves obtained with Gafchromic film. The origin of detector response differences was investigated by the approach to separately study the different effects that influence the signal: the volume effect, electron contamination, the effective point of measurement, and polarity effects.

2. MATERIALS AND METHODS

2.A. Depth dose curves using different detectors

Detector response in the buildup region was analyzed based on depth dose curves measured with different detectors. Depth dose curves were measured at a Primus linear accelerator (Siemens, Germany) at a beam quality of 6 MV in a MP3 water phantom using a Tandem Electrometer and Mephisto mc^2 acquisition software (all PTW Freiburg, Germany). A source to surface distance (SSD) of 100 cm was chosen for all measurements (Fig. 1). Depth dose curves were recorded for different square fields with nominal field sizes 10×10 cm^2, 4×4 cm^2, 2×2 cm^2, 1×1 cm^2, and 0.6×0.6 cm^2 at SSD 100 cm defined by MLCs in crossplane and jaws in inplane direction.

Different detectors, listed in Table I with their properties, were used. As a reference detector to account for the Linac output, a T-REF 34091 transmission chamber (PTW Freiburg, Germany) was positioned just below the collimator outlet leaving a gap of 47.5 cm between the T-REF and the water surface. Exemplary measurements were taken with and

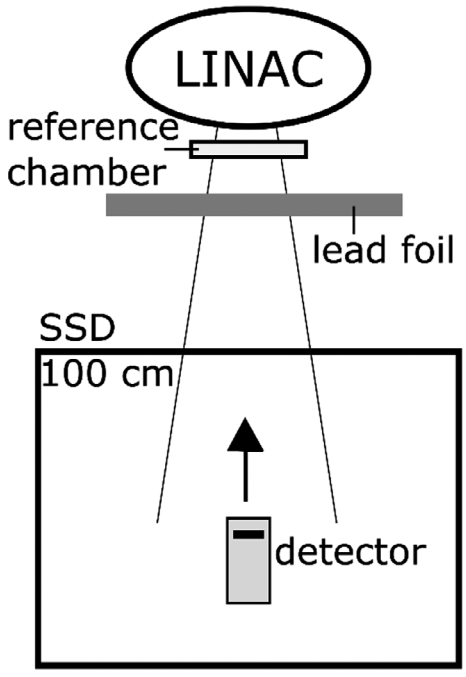

FIG. 1. Scheme of the experimental setup to measure depth dose curves. The lead foil close to the collimator outlet was only used in some experiments to study electron contamination. Detectors are either oriented parallel to the beam as shown in the picture (diodes except EDGE, microDiamond, plane-parallel detectors) or perpendicular to the beam (other ionization chambers, EDGE).

without the T-REF transmission chamber to quantify its effect in the buildup region using an unshielded diode PTW 60017 as the field detector.

For the results in the buildup region with its high dose gradients, detector positioning and setting the zero depth for each detector heavily influence the results. For lateral detector positioning, profiles were acquired for each detector, which was then moved into the field center. For the diodes and the microDiamond, the effective point of measurement was chosen according to the shifts suggested by the manufacturers. Those detectors were orientated parallel to the beam, except for the EDGE detector. For the plane-parallel chambers, the effective point of measurement was chosen at the back of the entrance window. The EDGE and the cylindrical ionization chambers were positioned with their stem perpendicular to the beam. For the cylindrical ionization chambers including the microchambers, the effective point of measurement was determined experimentally for each detector in a very similar way to the procedure suggested by McEwen et al.[17] A relative depth dose curve measured with each detector was shifted against a curve measured with a plane-parallel chamber, either a PPC40 for field sizes 10 × 10 and 4 × 4 cm^2 or a PPC05 for the field size 2 × 2 cm^2. Excluding the first 8 mm of the curves where detector differences are the largest, the shift that minimized the differences between the two curves was determined for each of the three field sizes and averaged, yielding the effective points of measurement (Table I).

The integration time per point was adjusted depending on the detector type and typically ranged from 0.2 to 5 s. All curves were measured at least three times per detector and normalized to the reading at 10 cm depth in water. The average and standard deviation from repeated measurements were calculated. For the small ionization chambers the size of the CC04 and below, measurements at positive and negative polarity were averaged. For larger ionization chamber, for example, the plane-parallel detectors, only measurements at positive polarity were considered. Additional lead shielding for the electrometer was used for all measurements to reduce effects of the scattered radiation reaching the electrometer, which has been shown to influence depth dose curves, especially for the smallest detectors.[18,19]

2.B. Film dosimetry

Depth dose curves were also recorded on EBT3 Gafchromic film (Ashland, USA). A single custom-cut piece of film was brought into the depth of interest and irradiated with the number of monitor units (MU) necessary to deposit a dose of approximately 2 Gy. Chosen depths for the irradiation were 200, 150, 100, 50, 40, 30, and 20 mm. Between 17 and 1 mm depth, a two millimeter interval was chosen. The measurements at each depth were carried out three times. The film holder was an approximately 3 × 4 cm^3 large PMMA frame. The film pieces were fastened to the holder for the measurements leaving the center of the film in contact with water. Six films per field size and depth were irradiated for the purpose of deriving the profiles.

Forty-eight hours after irradiation, the films were scanned using an Epson Expression 11000XL scanner with a transparency unit (Epson Seico, Japan), which was thoroughly warmed up. Films were consecutively placed in the same orientation in a central area of the scanner using a template. A glass compression plate was used to ensure a flat position of the films on the scanner surface. In each scan, two reference

TABLE I. Detectors used in this study, their properties according to manufacturer information and the shift used in this study to account for the effective point of measurement (EPOM). For ionization chambers, the shift refers to the fraction of the cavity radius r that the detector needs to be shifted from its reference point on the chamber axis toward the source.

Detector	Manufacturer	Radius of active volume (mm)	Thickness/length*of active volume (mm)	Comments	Position of EPOM
Diode 60012	PTW Freiburg, Germany	0.56	2.5 E-3	Unshielded	0.6 mm from front surface
SFD	Scanditronix, Sweden	0.3	60 E-3	Unshielded, stereotactic diode	0.5 mm from front surface
Razor Diode	iba Dosimetry, Germany	0.3	20 E-3	Unshielded, stereotactic diode	0.7 mm from front surface
Diode 60008	PTW Freiburg, Germany	0.56	2.5 E-3	Shielded	2.0 mm from front surface
PFD	Scanditronix, Sweden	1.0	60 E-3	Shielded, photon diode	0.5 mm from front surface
EDGE	Sun Nuclear Corporation, FL, USA	0.4	30 E-3	Diode, brass housing	0.3 mm from front surface
microDiamond 60019	PTW Freiburg, Germany	1.1	1 E-3		1 mm from front surface
FC23	iba Dosimetry, Germany	3.1	9*	Farmer type chamber	0.45r toward source
CC13	iba Dosimetry, Germany	3.0	5.8*		0.40r toward source
CC04	iba Dosimetry, Germany	2.0	3.6*		0.36r toward source
CC01	iba Dosimetry, Germany	1.0	3.6*		0.36r toward source
CC003	iba Dosimetry, Germany	1.0	2.0*		0.30r toward source
PPC05	iba Dosimetry, Germany	4.95	0.6	Plane-parallel chamber	0.3 mm into cavity from back of entry window
PPC40	iba Dosimetry, Germany	8	2	Plane-parallel chamber	Back of entry window

SFD, stereotactic diodes.

film pieces with known dose were present. Scans were taken with 150 dots per inch (dpi) resolution, eight times per film and saved in tagged image file (tif) format. As the scanner response was observed to be unstable during the first scans,[20] only the last five scans were averaged using MatLab (Mathworks, USA) before further processing the images.

Conversion of optical density into dose was carried out with the software FilmQA Pro (Ashland, USA) using the three-color method as proposed by Micke et al.[21] and the one-scan protocol.[22] The calibration curve used was obtained from irradiating several dose levels between 0 and 5.4 Gy in the water phantom under reference conditions. Different lots of EBT3 film (Lot 06081601 and 12121703) were used, but each with its own calibration curve.

Dose values of each film were either obtained by averaging over an area of approximately 5×5 mm^2 (10×10 and 4×4 cm^2 fields) or 4.2×4.2 mm^2 (2×2 cm^2 field) in the film center or by fitting a quadratic function around the peak of the dose distribution and extracting the maximum of the curve as the central dose (1×1 and 0.6×0.6 cm^2 fields).

Due to darkening of the reference films from repeated scanning, the dose values were corrected by an experimentally obtained correction linear with the number of previous scans. To obtain depth dose curves, the measurements from three individual films per depth were averaged. The ratio of dose per MU was calculated for each depth and normalized to the value at a depth of 100 mm.

A function borrowed from TPR curve fitting[23]

$$PDD(z) = (A + (1 - A)(1 - B^z)) * C \\ * \exp(-D * (1 - E * z) * z) \quad (1)$$

was fitted to each depth dose curve, which is a function of the depth z and was obtained with film at the positions mentioned above. Parameter A is the surface dose, which is field size dependent, B models the buildup gradient, C is a constant for normalization, and the exponential term with parameters D and E models the dose falloff.[23] The coefficient of determination R^2 was larger than 0.999 for all fitted curves. Results from the fit rather than the measured data points were used in the subsequent analysis to reduce noise.

2.C. Signal ratios

The signal ratio $SR(0,z)$ on the central field axis at depth z of a detector *Det* compared to film both measured at the same field size is calculated as

$$SR(0,z) = \frac{M_{Det}(0,z)/M_{Det}(0,z_{ref})}{M_{Film}(0,z)/M_{Film}(0,z_{ref})} \quad (2)$$

where M(0,z) is the measured signal and z_{ref} the reference depth chosen as 10 cm in water for this study. Assuming that film provides the correct dose-to-water, the signal ratio in the 10×10 cm^2 field is the inverse of the correction factor $k_\Omega(0,z,PDD)$ found in the literature, for example, in Francescon et al.[11] For all other field sizes, the signal ratios quantify the changes of detector response at different depths within the same field size. A separate treatment of each field size is advantageous for the application to measurements, where depth dose curves and output factors are typically measured independently.

The uncertainty of the signal ratios was calculated taking into account individual uncorrelated contributions: the standard deviation from repeated measurements of the same field with the same detector after completely new setups of the equipment, the deviation induced by a 0.1 mm detector positioning error in depth and by uncertainties from the film.

2.D. Influence of detector positioning

The choice of a different effective point of measurement changes the curve obtained with the detector, especially in the buildup region. Depth dose curves obtained with different detectors for the 10×10 cm^2 field as described in Section 2.A. were shifted on the depth axis and renormalized to the new 100 mm depth to create the following two curves: The PDD in which the EPOM is chosen at 0.5r from the chamber center according to the DIN protocol[24,25] and the PDD in which the EPOM is chosen according to Table I, which is the smaller shift used in this work. Ratios of the two curves were calculated. These can be interpreted as the change of the depth dose curve as a consequence of the chosen effective point of measurement.

2.E. Volume correction factors

Any detector with a finite size will experience volume averaging when the dose distribution is not homogeneous over its active volume. At depth, the field size increases due to the diverging beam. This results in a different amount of volume averaging. From film profiles, such a pure geometric volume effect can be derived for each plane taking into account how the dose profile changes laterally.[26] At any depth, we derived the volume correction of the given detector compared to a point measurement in the field center by using the proposed method of dividing the field into rings around the center. The fraction of the dose in each ring compared to the center of the field was then multiplied by the area of the ring and added up, yielding the volume effect in that plane. By deriving the volume effect at different depths and calculating their relation, the volume effect occurring for depth dose measurements due to the lateral dimensions of the detector can be accounted for.

2.F. Filtering out electron contamination

In order to quantify to which extent electron contamination in the photon beam contributed to detector response, a 25×25 cm^2 lead foil with a thickness of 1.5 mm was placed between the collimator and the water phantom just below the transmission chamber. Depth dose curves for selected detectors and field sizes were measured in pairs: one

measurement with the foil, one without the foil in arbitrary order one directly following the other. All other parameters were left as described in Section 2.A. Both curves were normalized to 100 mm depth and the ratio between the relative depth dose curves with and without the foil was calculated. Selected depths were sampled with film both with and without the foil.

2.G. Polarity effects

In order to quantify the polarity effect in the buildup region, curves with small ionization chambers were recorded at both polarities with a 0.2 mm step size from the surface to 18 mm depth and a 0.5 mm step size at higher depths in the 2×2 cm^2, 4×4 cm^2, and 10×10 cm^2 fields. Exemplary curves were measured with the plane-parallel chambers at both polarities. As described for the measurements above, shielding of the electrometer and sufficient preirradiation after a change of polarity was respected. Each curve was normalized to 100 mm depth and then the ratio of the curves obtained with different biasing voltages was calculated.

3. RESULTS

3.A. Depth-dependent correction factors

In some cases, depth dose curves measured with the different detectors differ from the curves recorded on film, especially in the buildup region (Fig. 2). The curves for the detectors CC13, FC23, PPC40, and PPC05 were not measured for field sizes smaller than 2×2 cm^2, where volume averaging effects heavily influence the results. In general, a field size dependence was observed, indicating that detector response compared to film increases from 10×10 cm^2 field size to 1×1 cm^2 field size and then declines for the smallest analyzed 0.6×0.6 cm^2 field. Whether a detector shows over-response or its signal is lower than that of the film, varies with detector type and studied field sizes (as detailed in Fig. 2), but some general observations can be made: In the larger fields (10×10 and 4×4 cm^2), the film and the larger ionization chambers CC13 [Fig. 2(i)] as well as the PPC40 chamber [Fig. 2(m)] show very good agreement even at the lowest depth studied. At 3 mm depth, the obtained corrections do not exceed 1%. At the field sizes 2×2 and 1×1 cm^2, the three small ionization chambers CC04, CC01, and CC003 [Figs. 2(j)–2(l)] over-respond in the buildup region. For the Razor Diode, the shielded diode PTW 60008 and the EDGE detector, the over-response increases even further with a maximum of 1.21 at a 1×1 cm^2 field for the diode 60008 at 3 mm depth. The unshielded diode PTW 60012, the SFD and the PFD have a response lower than film for some field sizes and a response higher than film for those of medium size. The spread of the corrections needed at different field sizes is larger for some detectors than for others. For example, the maximum difference between the corrections at 11 mm depth is 3.8% for the SFD and 2.9% for the Razor Detector, while it is only 1.8% for the EDGE and 1.4% for the microDiamond 60019 at the same depth.

Another point to be noted is the different slope of the curves at depth. While the depth dose curves of some detectors, namely the Razor Detector, SFD, Diode 60008, and the microDiamond, are very close to the film, visible as a correction factor close to 1, some detectors deviate, notably the diode PTW 60012 with a response ratio of 0.987 at 200 mm depth in a 10×10 cm^2 field [Fig. 2(a)] and the PFD with a response ratio of 1.022 [Fig. 2(e)].

Uncertainties of the stated corrections were estimated for each depth taking several influence parameters into account. The standard deviations from repeated measurements of the normalized curves described in Section 2.A were comparable for all field sizes and typically amounted to a few tenth of a percent, at maximum 0.6%. Doses on film in individual depths and field sizes were reproducible with a 1.2% standard deviation. Following the fit with Eq. (1), the uncertainty for the film depth dose curves was around 1% at all points except for the outermost data points with an estimated 2% at 3 mm depth and 3.5% in 200 mm depth for all field sizes. As only relative doses between films at different depths were included in the further analysis, further uncertainties from the film processing are negligible. The positional uncertainty of the depth setting with different detectors, described in Section 2.D, compared to the depth setting with the film resulted in uncertainties of the calculated signal ratios smaller than 0.5% at depths 11 mm and deeper and negligible near the dose maximum. At 3 mm depth, the uncertainty was 3.4%. These three major contributions are comparable for all studied field sizes and detectors, so generic values for the uncertainties are stated for all field sizes and detectors. All three quantities are uncorrelated and yield a combined uncertainty that depends on the depth and is 3.1% at 3 mm depth, 1.3% at 5 mm depth, 0.5% at 17 mm depth, 0.9% at 50 mm depth, and 3.5% at 200 mm depth. Other influence parameters, especially regarding the reproducibility of the field size, lateral detector positioning and the SSD are assumed to be implicitly included in the uncertainty from repeated measurements, when the equipment was setup independently. For reasons of visibility of the other data, uncertainties are only displayed for one set of data points [Fig. 2(g)]. The highest contribution to the uncertainty in the buildup region stems from the positioning, which increases the uncertainty as one approaches the surface.

A comparison of the depth dose curves acquired with different detectors and those recorded with EBT3 film using distance-to-agreement (DTA) analysis is shown for the buildup region in Fig. 3. While most detectors showed DTA below 0.2 mm, especially the shielded diodes yielded values of 0.5 mm and more.

3.B. Influence of detector positioning

The position of the detector relative to the water surface, and therefore the chosen effective point of measurement, influences the depth dose curves in the buildup region, while

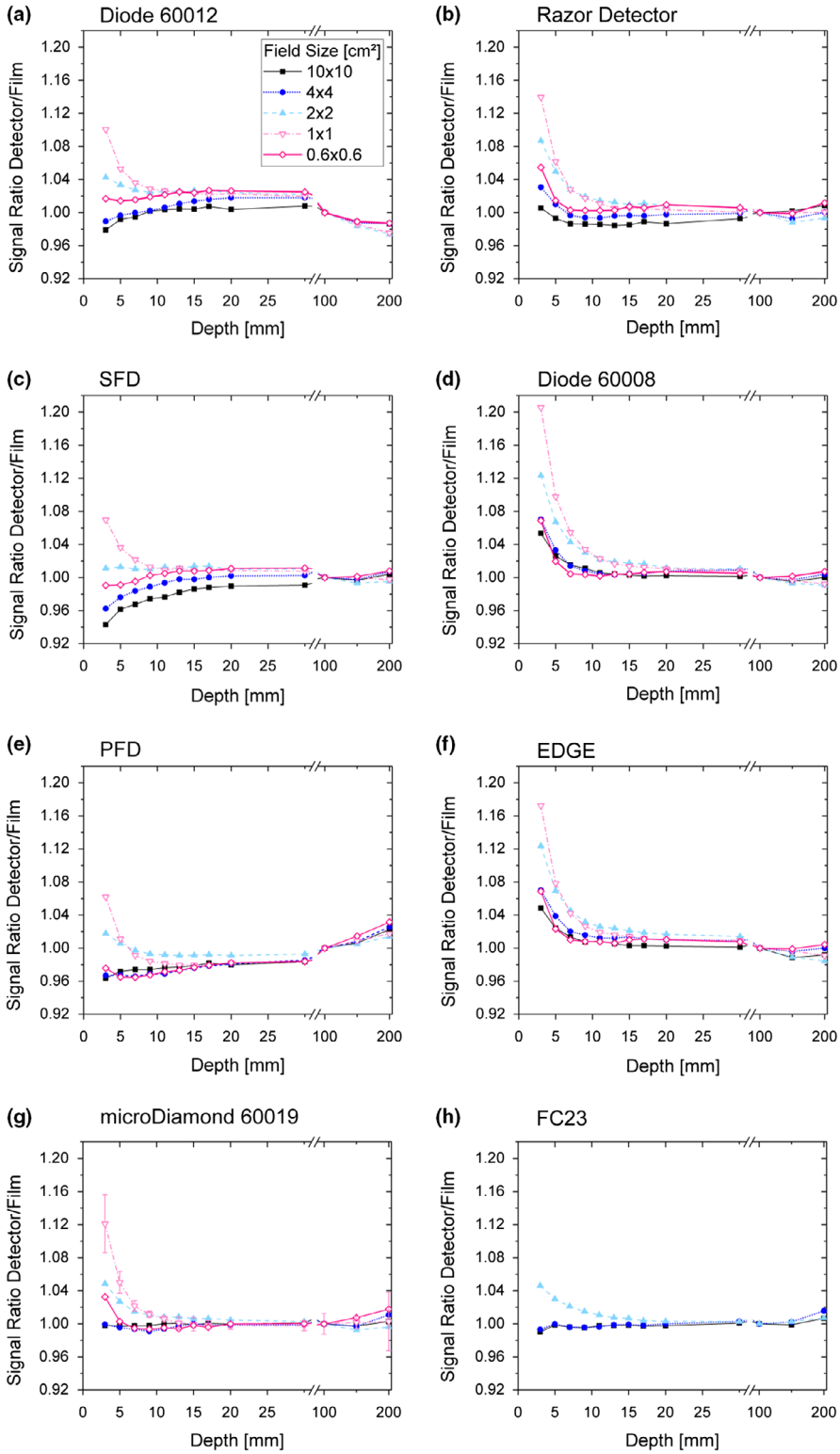

FIG. 2. Signal Ratios of different detectors relative to EBT3 Film as a function of depth for different field sizes. All curves are normalized to 10 cm depth. Uncertainties are given exemplary in (g). [Color figure can be viewed at wileyonlinelibrary.com]

it has negligible effect on the results at larger depth (Fig. 4). For all ionization chambers, the chosen EPOM shifts were smaller than 0.5 times the cavity radius. In the buildup region, especially <10 mm below the surface, this choice of the effective point of measurement smaller than 0.5r led to a reduction of the relative signal at a given depth in the buildup region of a few percent [Fig. 4(a)]. The ratios of the acquired relative dose values in the buildup region are further reduced when, instead of the individually derived shifts, no EPOM shift is applied [Fig. 4(b)].

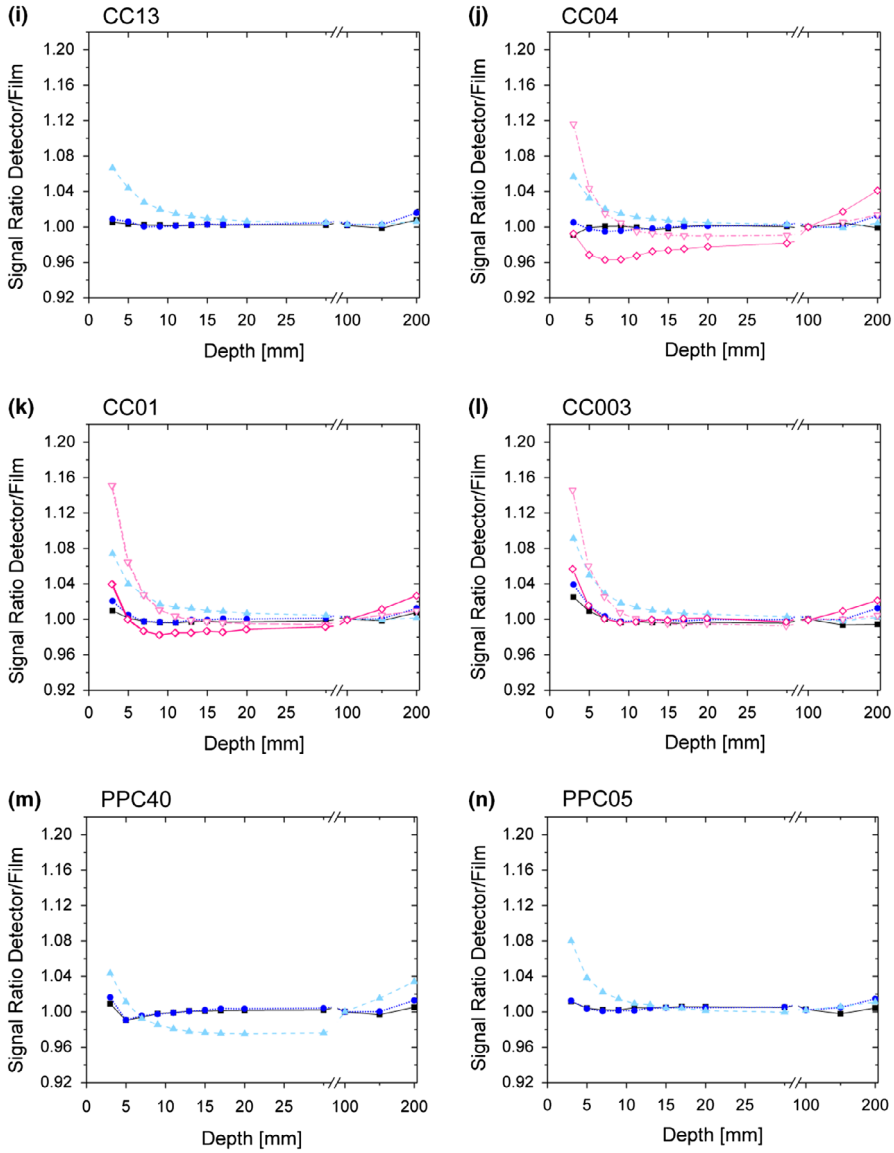

FIG. 2. Continued

3.C. Volume Correction Factors

Volume correction factors due to the lateral dimensions of a detector for different field sizes were derived and the values for the 0.6 × 0.6 cm^2 field are shown as an example in Fig. 5. As expected, the needed corrections increased with the detector size. For the size of the SFD (radius 0.3 mm), no corrections were necessary down to the 0.6 × 0.6 cm^2 field. For the size corresponding to the PTW diodes (r = 0.56 mm), corrections were also negligible with a maximum correction of 1.002 in that smallest field. For the size of a microDiamond (r = 1.1 mm), corrections in the 1 × 1 cm^2 field were still negligible, but in the 0.6 × 0.6 cm^2 field corrections up to 1.006 in the buildup region were found. More substantial corrections were necessary for larger detectors, for example for a detector sized as the PPC05 chamber (radius 5 mm), corrections were up to around 1.20 in the surface-near region in the 0.6 × 0.6 cm^2 field. Chambers the size of a PPC40 chamber (radius 8 mm) show a volume effect due to the lateral dimensions that need a correction of approximately 1.24 already at the depth of dose maximum and 1.32 at 3 mm depth in a 0.6 × 0.6 cm^2 field.

3.D. Electron contamination

The introduction of a lead foil into the beam path reduced the PDD signals in the buildup region for all detectors [Fig. 6(a)]. Film measurements are shown for the three lowest depths. The decline was detector-type specific. While the response of the shielded diodes 60008, PFD, and EDGE was reduced by approximately 2% at 3 mm depth, the response of most of the other diodes was typically reduced by around 3% at that depth. At 20 cm depth, the relative depth dose curve increased for all detectors by around 0.5% with foil compared

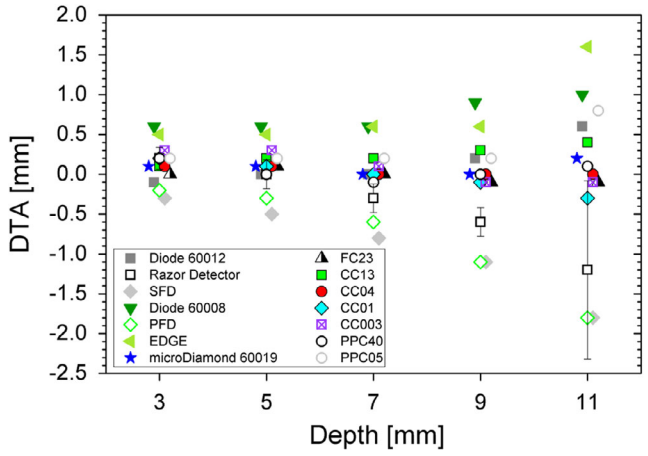

FIG. 3. Comparison of depth dose curves of different detectors with EBT3 in a 10 × 10 cm^2 field evaluated by distance-to-agreement (DTA), where negative DTA indicate lower signal ratios than the film. For better visibility, points are spaced out around the indicated depth. Uncertainties are shown exemplary for one detector. [Color figure can be viewed at wileyonlinelibrary.com]

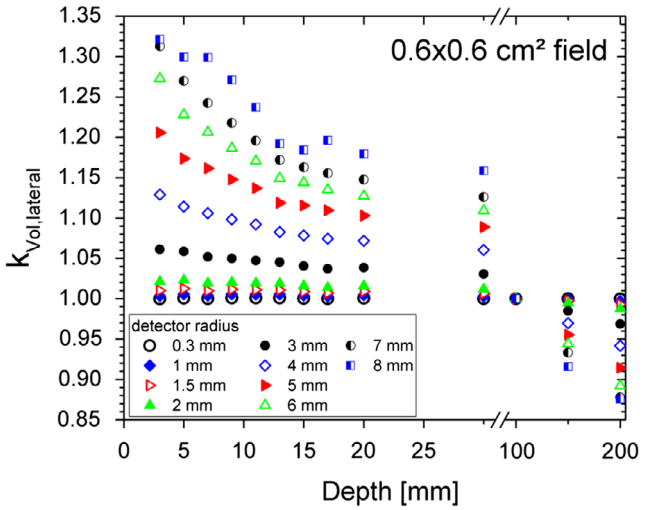

FIG. 5. Geometric volume correction factors as a function of depth to correct depth dose curves for the lateral size of detectors with different radii for the 0.6 × 0.6 cm^2 field. [Color figure can be viewed at wileyonlinelibrary.com]

to no foil. As the curves without the foil always included the T-ref chamber as a reference and we found differences between curves with and without the detector, all values for electron contamination can only be stated with an uncertainty of around 1%.

The same trends for the different field sizes were observed for all detectors. The curves of one detector are shown as an example in Fig. 6(b). The effect of the lead foil in the buildup region is the largest in the largest field and then reduces with field size. At 3 mm depth, the ratio changes from 0.962 at 10 × 10 cm^2 field size to 0.979 at 1 × 1 cm^2 field size.

3.E. Polarity effects in the buildup region

All stated corrections for the small ionization chambers (Fig. 2) refer to measurements averaging between both biasing voltages. The differences between depth dose curves measured at the respective polarities are shown in Fig. 7. The 10 × 10 cm^2 field is displayed, the measurements in all other studied field sizes yielded similar or smaller polarity effects.

The highest polarity effects were seen for the two smallest ionization chambers. A ratio between the depth dose curves measured at different polarities of 0.88 for the CC003 and 0.94 for the CC01 at 3 mm depth was found. For the larger ionization chambers, the ratios did not change more than 2% at 3 mm and larger depths. For the plane-parallel chambers, the ratio of the curves obtained at the different polarities did not deviate more than 1.5% from unity at all depth.

4. DISCUSSION

4.A. Correction factors

All studied detectors respond differently from film, that is, no ideal detector could be identified. For the 10 × 10 and 4 × 4 cm^2 field size, depth dose curves comparable to film were recorded for some detectors, such as the plane-parallel chambers, the three largest ionization chambers, and the microDiamond. However, at smaller field sizes most detector signals deviated considerably from the film in the buildup

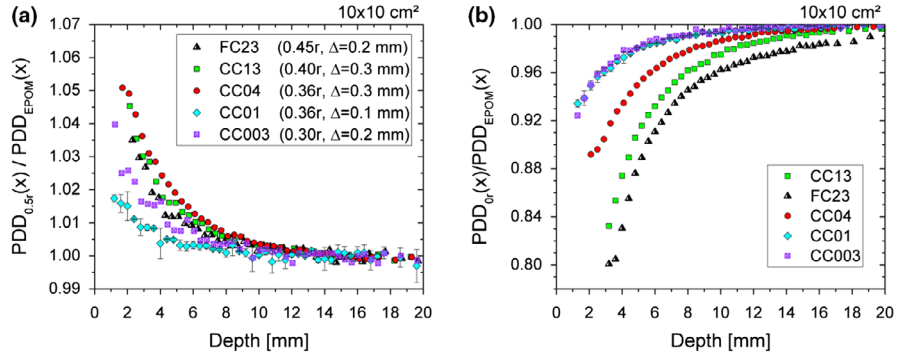

FIG. 4. Changes in the depth dose curves as a function of depth in a 10 × 10 cm^2 field. (a) When an EPOM shift of 0.5r for ionization chambers is chosen instead of the detector-individually derived effective point of measurement as tabulated in Table I. Δ is the difference in shift between 0.5r and the shift chosen in this work. (b) When the chamber axis is chosen as the EPOM instead of the detector-individually derived effective point of measurement. Uncertainties are shown exemplary for one detector only and are comparable for the others. [Color figure can be viewed at wileyonlinelibrary.com]

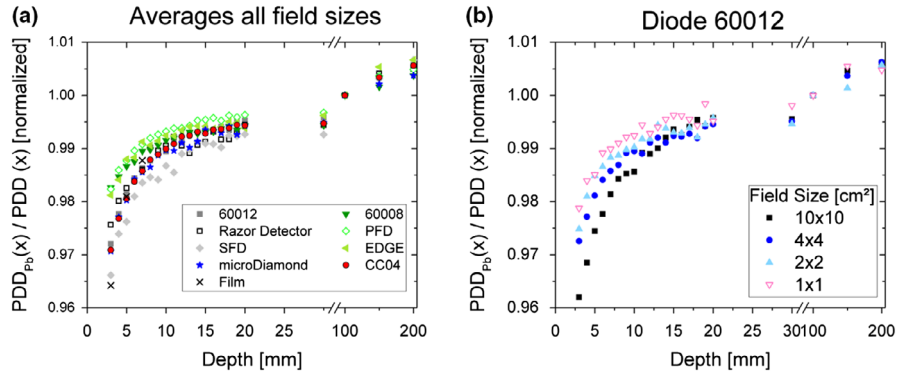

FIG. 6. Changes in the depth dose curves due to a lead foil placed in the beam a. for different detectors averaged over all field sizes and b. for a selected detector to show the field size dependence that was similar for all studied detectors. [Color figure can be viewed at wileyonlinelibrary.com]

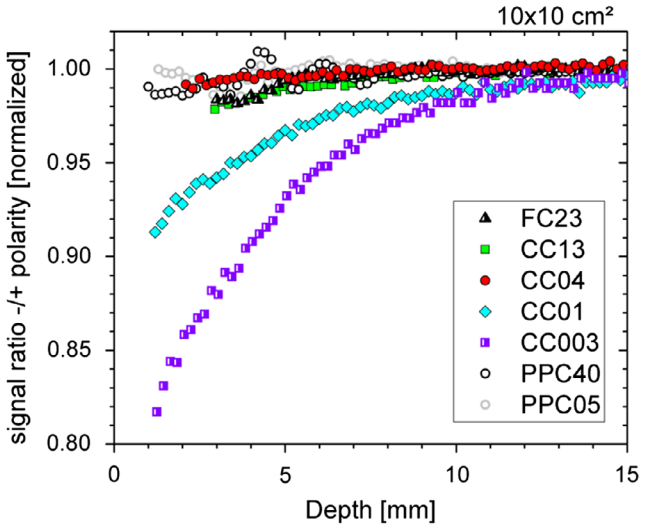

FIG. 7. Changes in the dose response as a function of depth induced by changing the sign of the biasing voltage for different ionization chambers in a 10 × 10 cm^2 field. [Color figure can be viewed at wileyonlinelibrary.com]

region (Fig. 2). As the buildup region is a high gradient region, small errors in detector positioning can lead to large differences in depth dose curves. Additional DTA analysis (Fig. 3) reveals whether the uncertainty in detector positioning can account for the observed detector response differences. The uncertainty associated with detector positioning is likely below 0.1 mm and at maximum 0.2 mm, including setting the depth of the detector at the water surface, the 0.1 mm step size of the water phantom and its reproducibility. DTA values increase toward the depth of dose maximum. In regions of low dose gradients, such as near the depth of dose maximum, a small change in dose corresponds to a larger DTA than closer to the surface. Therefore, the error bars in Fig. 3 are larger at depths around 11 to 15 mm than near the surface. DTA values decrease in the steep buildup region toward shallower depths. For most of the studied detectors, the differences in DTAs are at maximum 0.3 mm at 3 mm depth, indicating that the uncertainty in detector positioning cannot be the sole reason for the response differences here. The shielded diodes (PTW 6008, PFD) showed DTA of 0.5 mm to 0.6 mm at 3 mm depth. This means that the signal change corresponds to a positional change of 0.5 mm. Therefore, the observed differences for those detectors are clearly larger than the uncertainties.

Data for comparison obtained under the same conditions are scarce, but some depth-dependent detector signal correction factors are provided in the literature. Depth-dependent correction factors $k_\Omega(0,z,PDD)$ for a range of detectors, including the iba Razor Diode, PTW 60012, SN EDGE, and iba CC01, from Monte Carlo simulations have been reported by Francescon.[11] For the sake of comparison, the signal ratios we presented can be calculated from the data as $SR(0,z) = \frac{k_\Omega(0,10cm,PDD)}{k_\Omega(0,z,PDD)}$. For the descending part of the depth dose, their results agree with ours, except for the EDGE detector. For shallower depths than the dose maximum, the results of that investigation and ours agree well for some, but are not consistent for all studied detectors. Near the surface, where their first data point for the 5 mm circular cone is at 2 mm depth, the iba diode over-response can be calculated from the data in Fig. 2(a) by Francescon et al.[11] to approximately 6%, while the other two diodes would be around 3.5% (PTW 60012) to 4% (SN EDGE). Our results at 3 mm depth in the 0.6 × 0.6 cm^2 field are 5.5% for the iba Razor Diode (similar), 1.5% for the PTW 60012 (lower) and 6.9% (higher) for the SN EDGE. For the iba CC01 data by Francescon *et al.* indicated an underestimation of the signal below the surface by about 7% in their Fig. 2(b),[11] while we found an over-response of 4.0% at 3 mm depth. The trends of ionization chambers showing under-response and diodes over-response were also reported in a second study by the same first author.[16] It must be noted, that the investigations by Francescon *et al.* were done for a CyberKnife machine. No flattening filter is employed and cones were used as beam limiting devices in some of the measurements. Therefore, the photon spectrum and the abundance of electron contamination from machine parts will not be identical to the situation in a conventional medical linear accelerator. Differences observed for the ionization chambers are largely due to the different choice of the effective point of measurement shifts in their study and ours. For the very steep depth dose curve within the first few millimeters below the surface, even small changes of the positioning can have a huge effect. Using Fig. 4(b), the

above-mentioned under-response of 7% at 2 mm depth for the iba CC01 evident in the data provided by Francescon *et al*. reduces to 1.4% under-response when the EPOM is chosen as in our Table I. This mitigates the difference between the data presented here and Francescon et al., such that they agree within the uncertainties. For the diodes, the same effective point of measurement was used.

We observed an increasing over-response from larger to smaller field sizes until 1×1 cm^2 field size for all studied detectors. For the 0.6×0.6 cm^2 field, the signal ratio decreased considerably, typically about 10% at 3 mm depth (Fig. 2). The reason for this may be, that the majority or all electrons impinging the sensitive volume laterally originate in the detector housing or detector wall at this extremely small field. From data displayed in Fig. 3(a) of Francescon et al.,[11] a dependence on the field size can be deduced from the depth dependences of the correction factors, which follows the same pattern in the buildup region although with smaller differences between the field sizes.

Our curves in Figs. 2(a)2(f) illustrate that some diodes do not show the correct slope at depths. Thus, this investigation confirms that special care is necessary when attempting to measure depth dose curves with certain diodes. Over-response by 4% for the iba Razor diode at 300 mm depth was reported in a 11.5×10 cm^2 field.[16] We did not see noticeable depth dependence for both stereotactic diodes (SFD and Razor Diode) at large depths until a depth of 200 mm for relative depth dose curves when normalizing each curve separately. Yet we saw such dependence for some of the other diodes, for example, diode PTW 60012 and the PFD. Between the depth of dose maximum and 100 mm depth, the choice of the detector does have an effect that needs corrections smaller than 3% for all studied detectors and field sizes. In most cases, the corrections are even smaller. For the microDiamond, maximum corrections are 0.6%.

Very close to the surface the choice of the detector heavily influences the results. The highest deviations are present for some of the diodes. The shielded diode 60008 and the EDGE show over-response in the buildup region already for the larger field sizes 2×2 to 10×10 cm^2. Unshielded diodes, the microDiamond or small-sized ionization chambers seem to be equally good in the buildup region even in small fields. For the complete depth dose curve, the microDiamond or one of the small ionization chambers CC01 and CC003 averaged between both polarities seems to be a good choice in small fields. Above the 2×2 cm^2 field size a CC13 scanning chamber, and above a 4×4 cm^2 field size the PPC40 are valid choices both at depth and in the buildup region. Care should be taken with some of the shielded diodes, as 60008 showed a large over-response in the buildup region and PFD exhibited over-response at larger depths.

As in any other situations without charged particle equilibrium, deviations between the signals from film and the different detectors can be expected in the buildup region. Close to the surface, electrons reaching the detector will be largely coming in from the side or as backscatter, as there is only little material between the detector and the air. Detector response in a more extreme situation, in which the central part of the beam was blocked out, was studied previously.[27] There, all diode detectors were found to considerably over-respond to scattered radiation when the field size decreased below 15 mm. Similarly, in this study the over-response was present at the surface of the smaller fields, especially for the 1×1 cm^2 field.

Although the type A uncertainty for Gafchromic film is quite high, its high degree of energy independence, its negligible fluence perturbation, and its high spatial resolution make it the ideal reference detector. With our proven film protocol and by sufficient repetition statistically significant results were achieved. A small energy dependence was observed for EBT3 film, for example by Massillon-JL[28] or Butson,[29] which might also change from lot to lot. In our measurements (Fig. 2) it was confirmed that the film, the PPC40 and larger ionization chambers showed very good agreement in the larger field sizes, giving credibility to the film and rendering any bigger effects due to the energy dependence unlikely.

A possible influence from the transmission detector T-REF could be ruled out: The detector was placed in the beam path very close to the collimator as far away from the water surface as possible. The difference between the normalized depth dose curves with and without the T-REF transmission detector did not exceed 1% at all parts of the curve, including the buildup region.

4.B. Influence of detector positioning

Detector positioning considerably affects the obtained depth dose curves in the buildup region with a high dose gradient. Measurement uncertainties especially stem from the definition of the detector position at depth zero. Even a small shift of the order of 0.2 mm can lead to a change in response of the order of a few percent very close to the surface. In another work, we obtained individual effective points of measurement for all ionization chamber.[30] These values were used here and they differ from the canonical 0.5 or 0.6 times the cavity radius by a few tens of a millimeter. Therefore, to obtain reasonable data in the buildup region, it is necessary to use a chamber type specific effective point of measurement or to shift the recorded curves accordingly. This was also suggested by McEwen et al.[17] The larger the shift of the effective point of measurement, the larger was the resulting change on the depth dose curve. Consequently, differences between the shifted and the unshifted curves [Fig. 4(b)] are bigger for detectors with larger radii (FC23, CC13) than for smaller detectors (CC01, CC003).

The large effects of the position of the effective point of measurement on the depth dose curves may also be an issue for the diode detectors. The over-response near the surface for the shielded diodes may be mitigated by choosing another effective point of measurement than indicated by the manufacturer. The consideration of the water-equivalent window thickness instead of the physical depth stated for the reference point is a simple possibility. However, in case of the diode

PTW 60008, the reference point is at 2 mm depth, the water-equivalent window thickness is 2.2 mm according to manufacturer information. A shift of only 0.2 mm of its depth dose curve reduces the over-response by 1% at 5 mm depth. While this correction is in the desired direction, it is still small compared to the observed over-response.

Other authors already dismissed the thought of applying correction factors for depth dose measurements due to multi-dimensional factor dependencies, for example field size and depth.[16] As the positioning of the detectors is crucial for the results, there is an additional uncertainty associated with multiplying the readings of a detector with depth-dependent corrections. In our experiments, we found that the detector positioning was very reliable between repeated measurements. Yet it is questionable in how far different users define the depth in the same way and can use correction factors provided by someone else.

Our results suggest that there is no single detector providing accurate measurements for all field sizes in the buildup region. Yet some detectors seem to be more suitable than others. For practical purposes, we suggest following the TRS-483 concept of using more than one preferred detector for measurements.

4.C. Volume effect

To account for the lateral dimensions of the detectors, geometric volume correction factors were derived. Corrections remained negligible for the stereotactic diodes. Similarly, correction factors did not exceed 1.006 for detectors with a radius of 1 mm. The height of diodes' sensitive volumes is only a few micrometers, and can, therefore, be neglected. It is thus obvious, that the geometric volume effect alone has negligible influence on the response of the used diode detectors due to their small size. It can be concluded that other effects than volume averaging cause the need for the observed correction factors.

For ionization chambers with larger dimensions, the magnitude of the volume effect increases. The corrections suggest that volume averaging in the lateral direction excludes the PPC40 chamber as a suitable detector for depth dose curves in fields smaller than 2×2 cm^2 and the PPC05 chamber in fields below 1×1 cm^2. These deviations are visible in Fig. 2(m), where the 2×2 cm^2 corrections for the PPC40 chamber already deviate from the behavior at larger field sizes. For smaller ionization chambers, for example the CC04 to CC003, the volume averaging corrections are so small that they cannot account for the large detector signal differences observed in the buildup region.

4.D. Electron contamination

Another hypothesis was the electron contamination affecting the detector response, which was investigated by introducing the lead foil into the beam path. Using the lead foil to reduce contaminating electrons and very low-energy photons is expected to result in different depth dose curves due to the removed low-energy end of the spectrum: A decreasing slope at depth as well as a reduced signal in small depths. Especially diode over-response to low-energy photons is a well-investigated phenomenon,[31,32] leading to different responses of shielded and unshielded detectors in the buildup region.

In the experiment, these expectations were verified. The signal at 20 cm depth increased by approximately 0.5% for all detectors. The relative dose in the buildup region decreased. The fraction of the dose in the buildup region that originates from electron contribution reported by others is similar. For example an electron contribution of approximately 4% of the maximum dose at 4 mm depth for a 6 MV beam from a Siemens linac was reported.[33] Systematic differences between the detector types were visible. Shielded diodes were less affected from the introduction of the foil. The unshielded diodes' response was reduced more, indicating that they initially showed an over-response to contaminating electrons, or possibly the low-energy photons, present in the beam without the foil. A field size dependence was observed, leading to a higher reduction of the signal with the foil in larger fields than in smaller ones. Assuming the removal of contaminating electrons to be the cause for the reduction, it is reasonable that more such electrons will be present in large fields escaping through the wider opening of the beam limiting devices.

We observed the changes in detector response due to the foil to be rather small with changes of the PDDs by 3% and 2% in the buildup region for the unshielded and shielded diodes, respectively. This observation cannot explain the different correction factors of the two diode types obtained in Fig. 2. There, especially the shielded diodes 60008 and the EDGE showed over-response more than 1% higher than the unshielded diodes. Additionally, the overall effects due to the foil are small compared to the observed deviations from the film and cannot provide an explanation for the obtained field size-dependent corrections in Fig. 2.

4.E. Polarity effects

While it is no concern for larger ionization chambers, for microchambers clear differences between the curves obtained with negative and positive biasing voltage were observed. Taking averages of polarity readings is recommended for small ionization chambers in small field dosimetry, especially at points where charged particle equilibrium does not exist. For plane-parallel ionization chambers, polarity effects are known to increase in the buildup region of photon beams depending on the chamber design parameters.[34,35] This is explained by electrons being ejected in the forward direction when a photon beam hits the collecting electrode, leaving it with a positive charge at the site of the interaction.[34,35] This influences the resulting voltages present in the chamber, in a different way for each polarity. The effect is reduced at depth where the charge is compensated by electrons produced in the medium above and stopping at the collector. This model can also account for the high polarity effect observed in small ionization chambers just below the water surface.

The two smallest studied chambers CC01 and CC003 showed the largest polarity effects in the buildup region, while the larger CC04 showed hardly any differences between the polarities. Irradiation of the central electrode and cables is known to influence the polarity effect.[36] Different materials are used for the inner electrodes of those detectors, Shonka for the CC04, steel for the CC01 and graphite for the CC003. It is necessary to average between both polarities in the surface-near region even for relative measurements for chambers smaller than the CC04. Otherwise, the introduction of huge deviations of 10% or more in the buildup region is possible.

5. CONCLUSIONS

Depth dose curves for different detector types were measured and compared to Gafchromic film. Special emphasis was placed on the buildup region, where large corrections are necessary in some cases. The highest deviations were observed among the shielded diodes.

The geometric volume effect was estimated from film measurements in planes at different depths and shown to play a minor role for small detectors, such as diodes or small ionization chambers.

The response to contaminating electrons or low-energy photons of the different detectors showed a small detector-type dependent trend. Removing such contamination with a lead foil, the unshielded diode signal was reduced by about a percent more than the shielded diode signal. But the overall reduction of 2% compared to 3% at 3 mm depth does not constitute a decisive factor for their response in the buildup region.

Most crucial for the response factor was the detector position relative to the surface. Small detector shifts were shown to introduce large changes in the buildup region. Therefore, detector specific values for the effective points of measurements should be taken into account, which is feasible for ionization chambers.

When using small-sized ionization chambers, polarity effects can heavily influence the detector response and easily show differences near the surface of more than 10% between opposing signs of the biasing voltage. It therefore is unavoidable to measure curves at both polarities and average them.

None of the studied detectors can be recommended for measurements in the buildup region in all field sizes without restrictions. The best detector choices yielding correct curves at all depths and requiring the smallest corrections near the surface are the microDiamond 60019 and the two small ionization chambers CC01 and CC003 for all of the studied field sizes from 0.6×0.6 cm^2 to 10×10 cm^2. The response of shielded diodes depended on the type. Here, the shielded diode 60008 required the highest corrections. In general, unshielded diodes should be preferred over shielded ones. Ideally, one should back up the measurements in the buildup region with a second detector of a different type and be aware of the presence and magnitude of remaining systematic deviations.

ACKNOWLEDGMENTS

The authors thank iba Dosimetry for the loan of several ionization chambers used in this work. Sonja Wegener was supported by Deutsche Forschungsgemeinschaft (DFG) grant SA 481/10-1.

CONFLICT OF INTEREST

Barbara Herzog is now employed by iba Dosimetry, but was not during the time the study was carried out.

[a)]Author to whom correspondence should be addressed. Electronic mail: wegener_s1@ukw.de.

REFERENCES

1. Chung H, Jin H, Dempsey JF, et al. Evaluation of surface and build-up region dose for intensity-modulated radiation therapy in head and neck cancer. *Med Phys*. 2005;32:2682–2689.
2. Ramsey CR, Seibert RM, Robison B, Mitchell M. Helical tomotherapy superficial dose measurements. *Med Phys*. 2007;34:3286–3293.
3. Hsu S-H, Moran JM, Chen Y, Kulasekere R, Roberson PL. Dose discrepancies in the buildup region and their impact on dose calculations for IMRT fields. *Med Phys*. 2010;37:2043–2053.
4. Abdel-Rahman W, Seuntjens JP, Verhaegen F, Deblois F, Podgorsak EB. Validation of Monte Carlo calculated surface doses for megavoltage photon beams. *Med Phys*. 2005;32:286–298.
5. IAEA. Dosimetry of Small Static Fields Used in External Beam Radiotherapy. In: Technical Reports Series No. 483 International Atomic Energy Agency, Vienna; 2017.
6. Gerbi BJ, Khan FM. Measurement of dose in the buildup region using fixed-separation plane-parallel ionization chambers. *Med Phys*. 1990;17:17–26.
7. Mellenberg DE Jr. Determination of build-up region over-response corrections for a Markus-type chamber. *Med Phys*. 1990;17:1041–1044.
8. Nilsson B. Electron contamination from different materials in high energy photon beams. *Phys Med Biol*. 1985;30:139–151.
9. LaRiviere PD. Surface dose from 6 MV photon interactions in air. *Phys Med Biol*. 1983;28:285–287.
10. Das IJ, Cheng C-W, Watts RJ, et al. Accelerator beam data commissioning equipment and procedures: report of the TG-106 of the therapy physics committee of the AAPM. *Med Phys*. 2008;35:4186–4215.
11. Francescon P, Beddar S, Satariano N, Das IJ. Variation of kQclin, Qmsr-fclin, fmsr for the small-field dosimetric parameters percentage depth dose, tissue-maximum ratio, and off-axis ratio. *Med Phys*. 2014;41:101708.
12. Scherf C, Peter C, Moog J, et al. Silicon diodes as an alternative to diamond detectors for depth dose curves and profile measurements of photon and electron radiation. *Strahlenther Onkol*. 2009;185:530–536.
13. Akbas U, Donmez Kesen N, Koksal C, Bilge H. Surface and buildup region dose measurements with markus parallel-plate ionization chamber, GafChromic EBT3 Film, and MOSFET detector for high-energy photon beams. *Adv High Energy Phys*. 2016;2016:1–10.
14. O'Shea E, McCavana P. Review of surface dose detectors in radiotherapy. *J Radiother Pract*. 2006;3:69–76.
15. Apipunyasopon L, Srisatit S, Phaisangittisakul N. An investigation of the depth dose in the build-up region, and surface dose for a 6-MV therapeutic photon beam: Monte Carlo simulation and measurements. *J Rad Res*. 2013;54:374–382.
16. Francescon P, Kilby W, Noll JM, Masi L, Satariano N, Russo S. Monte Carlo simulated corrections for beam commissioning measurements with circular and MLC shaped fields on the CyberKnife M6 System: a study including diode, microchamber, point scintillator, and synthetic microdiamond detectors. *Phys Med Biol*. 2017;62:1076–1095.

17. McEwen MR, Kawrakow I, Ross CK. The effective point of measurement of ionization chambers and the build-up anomaly in MV x-ray beams. *Med Phys*. 2008;35:950–958.
18. Sarkar V, Wang B, Zhao H, et al. Percent depth-dose distribution discrepancies from very small volume ion chambers. *J Appl Clin Med Phys/ Am Coll Med Phys*. 2015;16:432–442.
19. Wegener S, Sauer OA. Electrometer offset current due to scattered radiation. *J Appl Clin Med Phys*. 2018;19:274–281.
20. Paelinck L, De Neve W, De Wagter C. Precautions and strategies in using a commercial flatbed scanner for radiochromic film dosimetry. *Phys Med Biol*. 2007;52:231–242.
21. Micke A, Lewis DF, Yu X. Multichannel film dosimetry with nonuniformity correction. *Med Phys*. 2011;38:2523–2534.
22. Lewis D, Micke A, Yu X, Chan MF. An efficient protocol for radiochromic film dosimetry combining calibration and measurement in a single scan. *Med Phys*. 2012;39:6339–6350.
23. Sauer OA, Wilbert J. Functional representation of tissue phantom ratios for photon fields. *Med Phys*. 2009;36:5444–5450.
24. D. 6800-2:2008-3. Dosismessverfahren nach der Sondenmethode für Photonen- und Elektronenstrahlung - Teil 2: Dosimetrie hochenergetischer Photonen- und Elektronenstrahlung mitIonisationskammern; 2008.
25. Zakaria A, Schuette W, Younan C. Reference dosimetry according to the New German Protocol DIN 6800–2 and comparison with IAEA TRS 398 and AAPM TG 51. *Biomed Imaging Intervent J*. 2011;7:e15.
26. Ralston A, Tyler M, Liu P, McKenzie D, Suchowerska N. Over-response of synthetic microDiamond detectors in small radiation fields. *Phys Med Biol*. 2014;59:5873.
27. Wegener S, Sauer OA. Separation of scatter from small MV beams and its effect on detector response. *Med Phys*. 2017;44:1139–1148.
28. Massillon-JL G, Chiu-Tsao S, Domingo-Munoz I, Chan M. Energy sependence of the New Gafchromic EBT3 Film: dose response curves for 50 KV, 6 and 15 MV X-Ray Beams. *Int J Med Phys, Clin Eng Rad Oncol*. 2012;1:60–65.
29. Butson MJ, Cheung T, Yu PK. Weak energy dependence of EBT gafchromic film dose response in the 50 kVp-10 MVp X-ray range. *Appl Radiat Isot*. 2006;64:60–62.
30. Wegener S, Sauer OA. The effective point of measurement for depth-dose measurements in small MV photon beams with different detectors. *Med Phys*. 2019;46:5209–5215.
31. Griessbach I, Lapp M, Bohsung J, Gademann G, Harder D. Dosimetric characteristics of a new unshielded silicon diode and its application in clinical photon and electron beams. *Med Phys*. 2005;32:3750–3754.
32. Yarahmadi M, Wegener S, Sauer OA. Energy and field size dependence of a silicon diode designed for small-field dosimetry. *Med Phys*. 2017;44:1958–1964.
33. Sheikh-Bagheri D, Rogers DW. Monte Carlo calculation of nine megavoltage photon beam spectra using the BEAM code. *Med Phys*. 2002;29:391–402.
34. Gerbi BJ, Khan FM. The polarity effect for commercially available plane-parallel ionization chambers. *Med Phys*. 1987;14:210–215.
35. Johns HE, Aspin N, Baker RG. Currents Induced in the dielectrics of ionization chambers through the action of high-energy radiation. *Radiat Res*. 1958;9:573–588.
36. Looe HK, Büsing I, Tekin T, et al. The polarity effect of compact ionization chambers used for small field dosimetry. *Med Phys*. 2018;45:5608–5621.